

A Mathematical Model of Malaria Transmission Incorporating Four Optimal Control Strategies.

Abstract – Malaria is an endemic disease in many countries around the world and especially in Africa. In this paper, we developed and studied SEIR-SEI mathematical model for malaria with vertical transmission. The basic properties of the model were investigated. The next generation matrix approach was used to obtain the reproduction number, \mathcal{R}_0 , and discussed the existence of the endemic equilibrium. Furthermore, we applied four optimal control strategies to control the number of exposed and infected humans. These control strategies are: the use of treated bed nets, $u_1(t)$; intermittent prophylactic treatment in pregnancy, $u_2(t)$; prompt and effective case management, $u_3(t)$, and the use of insecticide spray, $u_4(t)$. According to our numerical simulation results, the use of all control strategies together is a very effective approach to reducing the number of exposed after some time and infected humans, while the number of recovered humans also increases. Moreover, the number of infected mosquitoes has also decreased. Thus, through these strategies together, we will be able to control the disease in a short period of time. These findings underscore the importance of timely and well-designed public health interventions in malaria outbreak scenarios.

Keywords – Malaria transmission; Vertical transmission; Numerical Simulation; Optimal control.

1. INTRODUCTION

Malaria is a life-threatening disease caused by *Plasmodium* parasites that are transmitted to humans through the bites of infected female Anopheles mosquitoes. In 2023, an estimated 263 million cases of malaria were reported globally, resulting in approximately 597,000 deaths. The African Region accounted for 94% of the total malaria cases and 95% of the associated deaths, underscoring its disproportionate burden of the disease. [1], [2]. There are five species of *Plasmodium* that can infect humans they are: *P.falciparum*, *P.vivax*, *P.ovale*, *P.malariae* and *P.knowlesi*. Among these species of human malaria parasites, *P.falciparum* is the most serious one [3], [4]. Globally, in 2023, malaria was estimated to have caused approximately 597,000 deaths, corresponding to a mortality rate of 13.7 per 100,000 population. This represents a steady decline from 2020, when the number of malaria deaths was estimated at 622,000 and the mortality rate stood at 14.9 per 100,000. The WHO African Region continues to bear the highest burden of malaria mortality, accounting for 95% of the estimated global malaria deaths. [1]. The estimated 228 million malaria cases was reported in the WHO African Region in 2020. Moreover, the case incidence reduced from 268 to 222 per 1000 population at risk between 2000-2019, but increased to 232 in 2020 mainly because of perturbations to services during the Covid-19 pandemic [5].

Mathematical models are essential tools that can be used to understand the behaviour and transmission of malaria. In addition to that, it can help in predicting the disease future and how we can prevent and control it. Several researchers have tried to control malaria disease through many optimal control strategies using mathematical approaches. Kazeem O.Okosun *et al* [7], studied and analyzed malaria transmission model using the treated bed nets, treatment of infective human and spray of insecticides as three control strategies to control and reduce the disease transmission with minimum cost. According to their simulation results the effective strategy for eliminating malaria is the combination between spray of insecticides and treatment of infective human. Gasper G.Mwanga *et al* [8], studied and discussed the optimal control practices and its strategies to control the malaria transmission using mathematical model with asymptomatic carriers of the disease and two age compartments of human population with four optimal control strategies. These

This footnote will be used only by the Editor and Associate Editors. The edition in this area is not permitted to the authors. This footnote must not be removed while editing the manuscript.

control strategies are: Long -Lasting treated mosquito nets, Indoor residual spraying, screening and treatment of infected individuals. Their simulation result shows that using the four optimal control together will reduce the malaria. Romero-Leiton *et al* [9], developed their model with three optimal control strategies: bed nets, intermittent prophylactic treatment in pregnancy and prompt and effective case management to eliminate the malaria in colombia. Their result shows that the death due to malaria and congenital transmission have important effects in the disease infection outcome [9]. M.Osman *et al*, studied the effects of incidence function in occurrence of phenomena of backward bifurcation in malaria transmission mathematical model and they formulated an optimal problem with three control strategies to control and reduce the disease transmission in Democratic Republic of Congo. Their control strategies included: Long-Last insecticide treated net $u_1(t)$, treatment with drug of infected human $u_2(t)$ and insecticide spray $u_3(t)$. Their optimal control simulation result shows that using $u_1(t)$ and $u_2(t)$ together is an effective strategy to reduce and control the infected human in the country [10]. Many of modern research papers has discussed the optimal control strategies of malaria and how to control and eliminate the disease including the co-infection of malaria with other diseases. For more information see [11]–[20]. In this paper, we modified the SEIR-SI models in [24] by adding the exposed class of mosquito population with progression rate from exposed mosquitoes to infected mosquitoes. Furthermore, we included to model [9], the insecticides spray as control strategy. Our target is to minimize the number of infected human with minimum cost.

This paper is organized as follows: In Section 2, we introduce the mathematical model that describes malaria transmission with vertical transmission and prove the positivity and boundness of the solutions. In section 3, we obtained the basic reproduction numbers and discussed the existence of disease-free and endemic equilibria. Numerical simulation of the model is presented in section 4. In section 5, we introduced four control strategies to model(1) with their analysis to reduce and control the disease (number of exposed and infected humans, as well as infected mosquitoes). Section 6, is devoted to the numerical analysis of optimal control strategies. Finally, the conclusion is given in section 7.

2. Mathematical Model

A. Model formulation

We modified the ordinary differential equations for the malaria transmission mode with vertical transmission [24], [25]. This is a standard SEIRS model for human and SEI for mosquito. The total population of human, N_h , is sub-divided into four compartments at time t , represented by Susceptible $S_h(t)$, Exposed $E_h(t)$, Infected $I_h(t)$, and Recovery $R_h(t)$ that means $N_h(t) = S_h(t) + E_h(t) + I_h(t) + R_h(t)$. Also, the total mosquito population, N_v , is sub-divided into three compartments at time t , they are Susceptible $S_v(t)$, Exposed $E_v(t)$, Infected $I_v(t)$ and $N_v(t) = S_v(t) + E_v(t) + I_v(t)$. We assumed that the susceptible humans and susceptible mosquitoes are recruited at constant rates, Λ_h and Λ_v , respectively. The probability of human infected due to the bite of an infected mosquito, ϕ , is β_h . The progression rate from exposed human $E_h(t)$ to infected human $I_h(t)$ is α_1 . Furthermore, $\frac{\psi}{2}$ represents the increase in susceptible humans due to birth of infected human and ψ represents the vertical transmission rate. Also, the progression rate from exposed mosquito $E_v(t)$ to infected mosquito $I_v(t)$ is α_2 and the probability of mosquito been infected is β_v . The rest of the model parameters are listed in Table (1) with their descriptions. From the above we have the following system

$$\left\{ \begin{array}{l} \frac{dS_h}{dt} = \Lambda_h + wR_h - \frac{\beta_h \phi I_v}{N_h} S_h - \mu_h S_h, \\ \frac{dE_h}{dt} = \frac{\beta_h \phi I_v}{N_h} S_h - (\alpha_1 + \mu_h) E_h, \\ \frac{dI_h}{dt} = \frac{\psi}{2} I_h + \alpha_1 E_h - (\delta + \rho + \mu_h) I_h, \\ \frac{dR_h}{dt} = \delta I_h - (w + \mu_h) R_h, \\ \frac{dS_v}{dt} = \Lambda_v - \frac{\beta_v \phi I_h}{N_v} S_v - \mu_v S_v, \\ \frac{dE_v}{dt} = \frac{\beta_v \phi I_h}{N_v} S_v - (\alpha_2 + \mu_v) E_v, \\ \frac{dI_v}{dt} = \alpha_2 E_v - \mu_v I_v, \end{array} \right. \quad (1)$$

With the initial conditions: $S_h(0) > 0, E_h(0) \geq 0, I_h(0) \geq 0, R_h(0) \geq 0, S_v(0) > 0, E_v(0) \geq 0, I_v(0) \geq 0$.

TAB. 1: Parameter values for model (1)

Parameter	Description	Value	Unit	Source
α_2	Exposed mosquitoes progression rate	0.055	Day ⁻¹	[7]
Λ_h	Humans recruitment rate	0.01	Humans \times Day ⁻¹	[26]
Λ_v	Mosquitoes recruitment rate	0.018	mosquitos \times Day ⁻¹	[26]
ϕ	Mosquitoes biting rate	0.3	Day ⁻¹	[27]
β_h	Humans transmission rate	0.70	Dimensionless	[26]
β_v	Mosquitoes transmission rate	0.20	Dimensionless	[26]
μ_h	Humans natural death rate	0.00102	Day ⁻¹	[26]
μ_v	Mosquitoes natural death rate	0.0039	Day ⁻¹	[26]
α_1	Exposed humans progression rate	0.10	Day ⁻¹	[26]
ψ	Vertical transmission rate	0.0091	Day ⁻¹	[26]
ρ	Disease induced death rate	0.0090	Day ⁻¹	Fitting
δ	Infection humans recovery rate	0.00297	Day ⁻¹	Fitting
w	Loss of immunity rate	0.00136	Day ⁻¹	[27]

B. Positivity and boundedness of the solutions

Lemma 1. Let $\rho^* = \frac{\psi - \rho}{\mu_h}$ and $n = \min(\frac{\Lambda_h}{\mu_h}, \frac{\Lambda_h}{\mu_h(1-\rho^*)})$ then the set Δ defined by

$\Delta = \left\{ (S_h, E_h, I_h, R_h, S_v, E_v, I_v) \in \mathbb{R}_+^7 : 0 \leq N_h \leq n, 0 \leq N_v \leq \frac{\Lambda_v}{\mu_v} \right\}$ is positively invariant with respect to the solution of the model (1) if $\rho^* < 1$. [24], [25]

Proof. By adding the first four equations of humans and the last three of the mosquitoes in (1) we obtain respectively.

$$\frac{dN_h}{dt} = \Lambda_h - \mu_h N_h + \mu_h \rho^* I_h, \quad (2)$$

$$\frac{dN_v}{dt} = \Lambda_v - \mu_v N_v, \quad (3)$$

from (2) clearly, if $\rho^* < 1$, then $\frac{dN_h}{dt} \leq \Lambda_h - \mu_h N_h$. Thus the solution is given by

$$N_h \leq \frac{\Lambda_h}{\mu_h} + (N_h(0) - \frac{\Lambda_h}{\mu_h}) e^{-\mu_h t}, \quad (4)$$

we verify that from (4) $N_h \leq \frac{\Lambda_h}{\mu_h}$ when $N_h(0) \leq \frac{\Lambda_h}{\mu_h}$. By substituting, $0 < \rho^* < 1$ when $I_h \leq N_h$ in (2) we get

$$\frac{dN_h}{dt} = \Lambda_h - (1 - \rho^*) \mu_h N_h, \quad (5)$$

by integrating equation (5) with respect to t , we obtain the following solution

$$N_h(t) \leq \frac{\Lambda_h}{\mu_h(1-\rho^*)} + (N_h(0) - \frac{\Lambda_h}{\mu_h(1-\rho^*)}) e^{-\mu_h(1-\rho^*)t}, \quad (6)$$

we observe obviously, $N_h(t) \leq \frac{\Lambda_h}{\mu_h(1-\rho^*)}$ when $N_h(0) \leq \frac{\Lambda_h}{\mu_h(1-\rho^*)}$. Consequently, we have $N_h(0) \leq n$. In addition to that, integrating equation (3) we get $N_v \leq \frac{\Lambda_v}{\mu_v}$. Finally, we conclude that the set is positively invariant with respect to the solution of model (1) under the condition $\rho^* < 1$ ■

3. Existence of equilibria

When $E_h = I_h = R_h = E_v = I_v = 0$, that means the model (1) has a disease-free equilibrium (DFE) D_0 , which is obtained by setting all the right hand sides of the system (1) to zero and its defined by $D_0 = (\frac{\Lambda_h}{\mu_h}, 0, 0, 0, \frac{\Lambda_v}{\mu_v}, 0, 0)$. According to the next generation matrix technique in [28], [29], we calculate the basic reproduction number of system (1) and it is given by:

$$\mathcal{R}_0 = \sqrt{\frac{\alpha_1 \alpha_2 \beta_h \beta_v \phi^2}{\mu_v (\alpha_1 + \mu_h) (\alpha_2 + \mu_v) (\mu_h (1 - \rho^*) + \delta)}}, \quad (7)$$

thus, we have the following lemma

Lemma 2. *The disease-free equilibrium (DFE) D_0 is locally asymptotically stable if $\mathcal{R}_0 < 1$ and unstable if $\mathcal{R}_0 > 1$.*

We assume that there exist an endemic equilibrium for model (1) denoted by:

$D^* = (S_h^*, E_h^*, I_h^*, R_h^*, S_v^*, E_v^*, I_v^*)$. Set all the right hand side of the model(1) equations to zero as:

$$\begin{cases} \Lambda_h + wR_h^* - \frac{\beta_h \phi I_v^*}{N_h^*} S_h^* - \mu_h S_h^* = 0, \\ \frac{\beta_h \phi I_v^*}{N_h^*} S_h^* - (\alpha_1 + \mu_h) E_h^* = 0, \\ \frac{\psi}{2} I_h^* + \alpha_1 E_h^* - (\delta + \rho + \mu_h) I_h^* = 0, \\ \delta I_h^* - (w + \mu_h) R_h^* = 0, \\ \Lambda_v - \frac{\beta_v \phi I_h^*}{N_v^*} S_v^* - \mu_v S_v^* = 0, \\ \frac{\beta_v \phi I_h^*}{N_v^*} S_v^* - (\alpha_2 + \mu_v) E_v^* = 0, \\ \alpha_2 E_v^* - \mu_v I_v^* = 0, \end{cases} \quad (8)$$

Then solve for $S_h^*, E_h^*, I_h^*, R_h^*, S_v^*, E_v^*$ and I_v^* , we obtain the following

$$\begin{aligned} S_h^* &= \frac{\Lambda_h \Lambda_v \alpha_1 \alpha_2 \beta_v \phi k_3 + (\Lambda_v \mu_v k_4 (\alpha_1 \delta w - k_2 (k_1 - \frac{\psi}{2})) - \Lambda_h \alpha_1 \beta_v \phi k_3 k_4 \mu_v) I_v^*}{\alpha_1 \beta_v \phi \mu_v k_3 (\alpha_2 \Lambda_v - \mu_v k_4 I_v^*)}, & E_h^* &= \frac{\Lambda_v \mu_v k_4 (k_1 - \frac{\psi}{2}) I_v^*}{\alpha_1 \beta_v \phi (\alpha_2 \Lambda_v - \mu_v k_4 I_v^*)}, \\ I_h^* &= \frac{\Lambda_v \mu_v k_4 I_v^*}{\beta_v \phi (\alpha_2 \Lambda_v - \mu_v k_4 I_v^*)}, & R_h^* &= \frac{\Lambda_v \mu_v \delta k_4 I_v^*}{\beta_v \phi k_3 (\alpha_2 \Lambda_v - \mu_v k_4 I_v^*)}, & S_v^* &= \frac{\Lambda_v \alpha_2 - \mu_v k_4 I_v^*}{\mu_v \alpha_2}, & E_v^* &= \frac{\mu_v I_v^*}{\alpha_2}, \end{aligned} \quad (9)$$

by adding the first two equations and substituting the points in (9) we obtain the equation

$$\beta_v \Lambda_h \Lambda_v \alpha_1 \alpha_2 \phi k_3 + (k_1 k_2 (1 - k_3) + \frac{\psi}{2} \Lambda_v \mu_v k_4 (k_1 k_3 - k_2) - \beta_v \Lambda_h \alpha_1 \phi \mu_v k_3 k_4) I_v^* = 0, \quad (10)$$

then we get $I_v^* = \frac{\beta_v \Lambda_h \Lambda_v \alpha_1 \alpha_2 \phi k_3}{\beta_v \Lambda_h \alpha_1 \phi \mu_v k_3 k_4 - \Lambda_v \mu_v k_4 (k_1 k_3 - k_2)}$, where $k_1 = (\delta + \rho + \mu_h)$, $k_2 = (\alpha_1 + \mu_h)$, $k_3 = (w + \mu_h)$ and $k_4 = (\alpha_2 + \mu_v)$. Thus, there exists one endemic equilibrium.

4. Numerical Simulation

In this section, based on the parameter values that are presented in Table(1), we carry out our numerical simulation using Matlab software. Fig.(1)(a) displays the solution of the model(1) for exposed $E_h(t)$, infected $I_h(t)$ and recovered humans $R_h(t)$ and the disease will decrease and after long time. Initially, there was a rapid rise in the infected population $I_h(t)$, peaking early before gradually declining over time. This indicates a fast spread of the infection. The recovered population, $R_h(t)$, increases over time as infected individuals recover, eventually surpassing the infected group. The exposed population, $E_h(t)$, also increases quickly in the early stages but remains lower in magnitude than the infected and recovered populations, indicating that exposure quickly transitions to infection. Fig.(1) (b), shows the solution of model(1) for susceptible $S_v(t)$, exposed $E_v(t)$, infected $I_v(t)$ respectively. Clearly, the susceptible mosquito population $S_v(t)$ drops sharply in the beginning as mosquitoes become exposed or infected. The infected mosquito population $I_v(t)$ increases significantly early on, peaking around day 250, then decreases steadily. The exposed mosquito population $E_v(t)$ remains relatively small, indicating a short incubation period before mosquitoes become infectious. In general, the simulations show how the disease spreads rapidly at first, driven by interactions between susceptible mosquitoes and infected humans, then gradually declines as populations develop immunity and interventions take effect. The system stabilizes over time with decreasing numbers of infected individuals and vectors.

Also, Fig.(1)(c) describes the influence of human transmission rate β_h . When the value of β_h is decreased, the number of infected humans $I_h(t)$ will also decrease accordingly. Clearly, from Fig.(1)(c) decreasing β_h will decrease the number of infected malaria cases and vice versa. Similarly, from Fig.(1)(d) increasing the value of the mosquitoes' transmission rate, β_v , will increase the infected individuals. Fig.(1) (e) shows the effect of the initial population of susceptible mosquitoes on infected humans, that is the number of infected humans increases according to increasing the initial conditions of mosquitoes. Furthermore, Fig.(1) (f) shows the effect of β_h, β_v, ϕ , and δ on the reproduction

number \mathcal{R}_0 . That is, increasing rates of (β_h, β_v, ϕ) amplifies the spread of infection. An increased infection recovery rate δ diminishes the epidemic potential.

To control and eliminate malaria, we have to reduce the transmission rates. To achieve this, we applied four control strategies to control the disease.

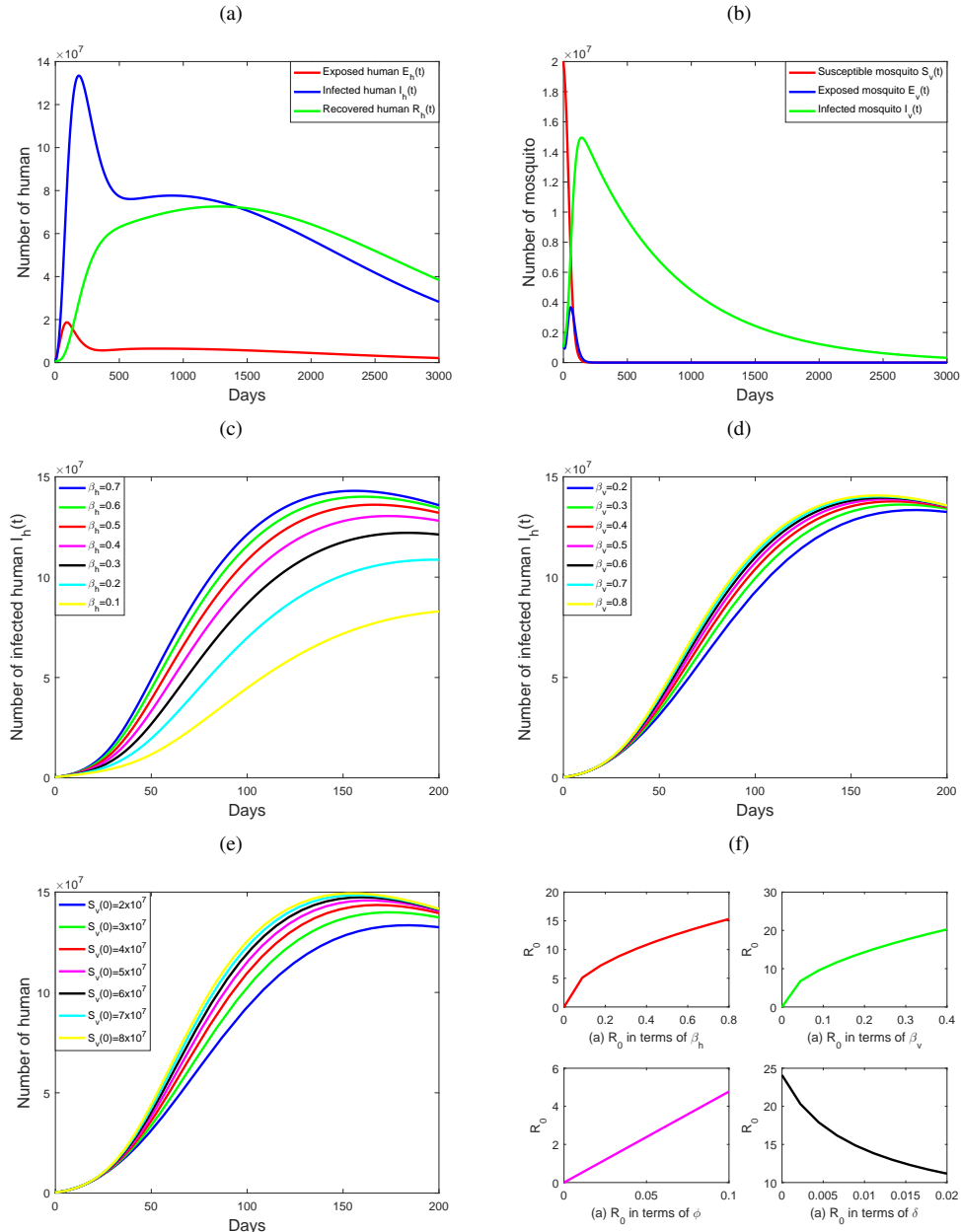


Fig. 1. (a) and (b) represent the solution of model (1) with parameter values from Table (1). (c) Represent the influence of β_h on the number of infected humans $I_h(t)$. (d) Represent the influence of β_v on the number of infected humans $I_h(t)$. (e) Represent the influence of S_v on the number of infected humans $I_h(t)$. (f) Represent the influence of $\beta_h, \beta_v, \phi, \delta$ on R_0 .

5. Optimal Control

In this section, we included four optimal control strategies to model(1). These controls are: the use of treated bed nets $u_1(t)$, intermittent prophylactic treatment in pregnancy $u_2(t)$, fast and effective case management $u_3(t)$, the use of insecticides $u_4(t)$, where $c_1 \in [0, 1]$ is the efficacy of the treatment and $c_2 \in [0, 1]$ is the efficacy of insecticides spray. From the above controls and all the assumption in model(1). We have the following equations

$$\left\{ \begin{array}{l} \frac{dS_h}{dt} = \Lambda_h + wR_h - (1 - u_1(t)) \frac{\beta_h \phi I_v}{N_h} S_h - \mu_h S_h, \\ \frac{dE_h}{dt} = (1 - u_1(t)) \frac{\beta_h \phi I_v}{N_h} S_h - (\alpha_1 + \mu_h) E_h, \\ \frac{dI_h}{dt} = (1 - u_2(t)) \frac{\psi}{2} I_h + \alpha_1 E_h - (\delta + \rho + c_1 u_3(t) + \mu_h) I_h, \\ \frac{dR_h}{dt} = (\delta + c_1 u_3(t)) I_h - (w + \mu_h) R_h, \\ \frac{dS_v}{dt} = \Lambda_v - (1 - u_1(t)) \frac{\beta_v \phi I_h}{N_v} S_v - (c_2 u_4(t) + \mu_v) S_v, \\ \frac{dE_v}{dt} = (1 - u_1(t)) \frac{\beta_v \phi I_h}{N_v} S_v - (\alpha_2 + c_2 u_4(t) + \mu_v) E_v, \\ \frac{dI_v}{dt} = \alpha_2 E_v - (c_2 u_4(t) + \mu_v) I_v, \end{array} \right. \quad (11)$$

our objective function is defined as:

$$J(u_1(t), u_2(t), u_3(t), u_4(t)) = \int_0^t (A_1 E_h + A_2 I_h + \frac{1}{2}(a_1 u_1^2(t) + a_2 u_2^2(t) + a_3 u_3^2(t) + a_4 u_4^2(t))) dt, \quad (12)$$

where A_1, A_2 represent balancing cost coefficients and a_1, a_2, a_3 and a_4 are the weighting constants for $u_1(t), u_2(t), u_3(t)$ and $u_4(t)$ respectively. We required an optimal control $u_1^*(t), u_2^*(t), u_3^*(t)$ and $u_4^*(t)$ such that:

$$J(u_1^*, u_2^*, u_3^*, u_4^*) = \min \{J(u_1, u_2, u_3, u_4) | u_1, u_2, u_3, u_4 \in \Upsilon\}, \quad (13)$$

where the control set $\Upsilon = \{(u_1, u_2, u_3, u_4) | u_i : [0, t_f] \rightarrow [0, 1], i = 1, 2, 3, 4\}$ is a Lebegue measurable set. The optimal system is considered with the necessary conditions that an optimal control should satisfy using Pontryagin's Maximum Principle [30]. It changes the model(11) and (12) into a problem of Hamiltonian principle H , pointwise with respect to optimal controls $u_1(t), u_2(t), u_3(t)$ and $u_4(t)$.

$$\begin{aligned} H = & A_1 E_h + A_2 I_h + \frac{a_1}{2} u_1^2(t) + \frac{a_2}{2} u_2^2(t) + \frac{a_3}{2} u_3^2(t) + \frac{a_4}{2} u_4^2(t) \\ & + \lambda_{S_h} \left\{ \Lambda_h + wR_h - (1 - u_1(t)) \frac{\beta_h \phi I_v}{N_h} S_h - \mu_h S_h \right\} \\ & + \lambda_{E_h} \left\{ (1 - u_1(t)) \frac{\beta_h \phi I_v}{N_h} S_h - (\alpha_1 + \mu_h) E_h \right\} \\ & + \lambda_{I_h} \left\{ (1 - u_2(t)) \frac{\psi}{2} I_h + \alpha_1 E_h - (\delta + \rho + c_1 u_3(t) + \mu_h) I_h \right\} \\ & + \lambda_{R_h} \left\{ (\delta + c_1 u_3(t)) I_h - (w + \mu_h) R_h \right\} \\ & + \lambda_{S_v} \left\{ \Lambda_v - (1 - u_1(t)) \frac{\beta_v \phi I_h}{N_v} S_v - (c_2 u_4(t) + \mu_v) S_v \right\} \\ & + \lambda_{E_v} \left\{ (1 - u_1(t)) \frac{\beta_v \phi I_h}{N_v} S_v - (\alpha_2 + c_2 u_4(t) + \mu_v) E_v \right\} \\ & + \lambda_{I_v} \left\{ \alpha_2 E_v - (c_2 u_4(t) + \mu_v) I_v \right\} \end{aligned} \quad (14)$$

Theorem 3. Assume the optimal controls $u_1^*, u_2^*, u_3^*, u_4^*$ and the solutions $S_h, E_h, I_h, R_h, S_v, E_v$ and I_v of corresponding state system (12), (13), that minimizes $J(u_1, u_2, u_3, u_4)$ over Υ . Then there exist adjoint variables $\lambda_{S_h}, \lambda_{E_h}, \lambda_{I_h}, \lambda_{R_h}, \lambda_{S_v}, \lambda_{E_v}, \lambda_{I_v}$ satisfying the following

$$-\frac{d\lambda_i}{dt} = \frac{\partial H}{\partial i}, \quad (15)$$

where $i = S_h, E_h, I_h, R_h, S_v, E_v, I_v$ with transversality conditions

$$\lambda_{S_h}(t_f) = \lambda_{E_h}(t_f) = \lambda_{I_h}(t_f) = \lambda_{R_h}(t_f) = \lambda_{S_v}(t_f) = \lambda_{E_v}(t_f) = \lambda_{I_v}(t_f) = 0, \quad (16)$$

and

$$\begin{aligned}
u_1^* &= \frac{1}{a_1} \left(\frac{\beta_h \phi I_v S_h}{N_h} (\lambda_{E_h} - \lambda_{S_h}) + \frac{\beta_v \phi I_h S_v}{N_v} (\lambda_{E_v} - \lambda_{S_v}) \right), \\
u_2^* &= \frac{1}{a_2} \frac{\psi}{2} I_h \lambda_{I_h}, \\
u_3^* &= \frac{c_1}{a_3} I_h (\lambda_{I_h} - \lambda_{R_h}), \\
u_4^* &= \frac{c_2}{a_4} (S_v \lambda_{S_v} + E_v \lambda_{E_v} + I_v \lambda_{I_v}),
\end{aligned}$$

Proof. Combined with the convexity of the integrand of $J(u_1, u_2, u_3, u_4)$ with respect to u_1, u_2, u_3 and u_4 , a priori bound of the state solutions, and the resulting Lipschitz characteristics of the state system (11), Theorem 4.1 and Corollary 4.1 of [30] guarantee the existence of an optimal control. Thus, the derivatives of H with respect to the adjoint variables are given by

$$\begin{aligned}
\frac{d\lambda_{S_h}}{dt} &= \mu_h \lambda_{S_h} + (1 - u_1(t)) \frac{\beta_h \phi I_v}{N_h} (\lambda_{S_h} - \lambda_{E_h}) + (1 - u_1(t)) \frac{\beta_h \phi I_v}{N_h^2} S_h (\lambda_{E_h} - \lambda_{S_h}) \\
\frac{d\lambda_{E_h}}{dt} &= -A_1 + (1 - u_1(t)) \frac{\beta_h \phi I_v}{N_h^2} S_h (\lambda_{E_h} - \lambda_{S_h}) + (\alpha_1 + \mu_h) \lambda_{E_h} - \alpha_1 \lambda_{I_h}, \\
\frac{d\lambda_{I_h}}{dt} &= -A_2 + (1 - u_1(t)) \frac{\beta_h \phi I_v}{N_h^2} S_h (\lambda_{E_h} - \lambda_{S_h}) + (1 - u_1(t)) \frac{\beta_v \phi}{N_v} S_v (\lambda_{S_v} - \lambda_{E_v}) \\
&\quad - (1 - u_2(t)) \frac{\psi}{2} \lambda_{I_h} - (\delta + \rho + c_1 u_3(t) + \mu_h) \lambda_{I_h} - (\delta + c_1 u_3(t)) \lambda_{R_h}, \\
\frac{d\lambda_{R_h}}{dt} &= (1 - u_1(t)) \frac{\beta_h \phi I_v}{N_h^2} (\lambda_{E_h} - \lambda_{S_h}) + (w + \mu_h) \lambda_{R_h} - w \lambda_{S_h}, \\
\frac{d\lambda_{S_v}}{dt} &= (1 - u_1(t)) \frac{\beta_v \phi I_h}{N_v} (\lambda_{S_v} - \lambda_{E_v}) + (1 - u_1(t)) \frac{\beta_v \phi I_h}{N_v^2} S_v (\lambda_{E_v} - \lambda_{S_v}) + (c_2 u_2(t) + \mu_v) \lambda_{S_v}, \\
\frac{d\lambda_{E_v}}{dt} &= (1 - u_1(t)) \frac{\beta_v \phi I_h}{N_v^2} S_v (\lambda_{E_v} - \lambda_{S_v}) + (c_2 u_4(t) + \alpha_2 + \mu_v) \lambda_{E_v} - \alpha_2 \lambda_{I_v}, \\
\frac{d\lambda_{I_v}}{dt} &= (1 - u_1(t)) \frac{\beta_h \phi}{N_h} S_h (\lambda_{S_h} - \lambda_{E_h}) + (1 - u_1(t)) \frac{\beta_v \phi I_h}{N_v^2} S_v (\lambda_{E_v} - \lambda_{S_v}) + (c_2 u_4(t) + \mu_v) \lambda_{I_v},
\end{aligned}$$

■

6. Numerical Simulation of Optimal Control

In this section, we discuss and analyze the numerical simulation of optimal control and the effects of our control strategies: the use of treated bed nets $u_1(t)$, intermittent prophylactic treatment in pregnancy $u_2(t)$, fast and effective case management $u_3(t)$, the use of insecticides $u_4(t)$, on model(1) using the parameter values that are provided in Table(1). We used approximately (5 months)140 days as the implementation time of our strategies with the initial conditions and applied the Runge-Kutta method of order four with Matlab software for the implementation of the graphs for the control strategies.

A. Combination of $u_2(t), u_3(t), u_4(t)$ together when $u_1(t)=0$

This is the strategy of applying intermittent prophylactic treatment in pregnancy $u_2(t)$, fast and effective case management $u_3(t)$ and the use of insecticides $u_4(t)$ together and set $u_1(t) = 0$. From Fig(2).(a) it can be seen that this strategy has no effect on the exposed humans. On the other hand, this strategy greatly increases the recovered humans as in Fig.(2)(c). In addition to that, the number of infected humans and infected mosquitoes has been highly increased, as in Fig(2).(b) and (d) respectively.

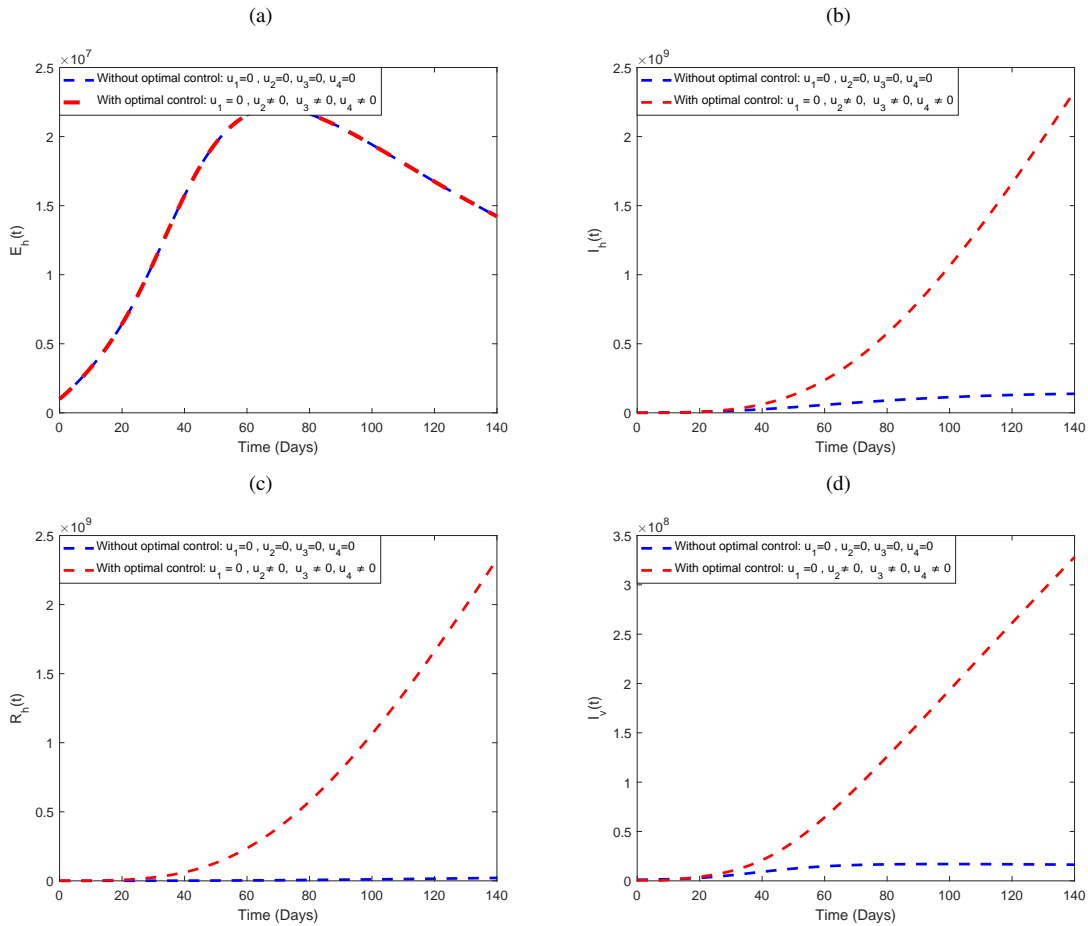


Fig. 2. (a), (b), (c), and (d) represent the behaviors of exposed, infected and recovered humans and infected mosquitoes respectively. Dashed blue line represents system without control ($u_1(t) = 0, u_2(t) = 0, u_3(t) = 0, u_4(t) = 0$) and Dashed red line shows the system with control ($u_1(t) = 0, u_2(t) \neq 0, u_3(t) \neq 0, u_4(t) \neq 0$.)

B. Combination of $u_1(t), u_3(t), u_4(t)$ together when $u_2(t) = 0$.

This is the strategy of using $u_1(t), u_3(t), u_4(t)$ together and setting $u_2(t) = 0$. This strategy significantly reduces the number of exposed humans until after day 110, and the number with control begins to increase again as in Fig.(3) (a). Also, increasing the number of infected and recovered humans and the number of infected mosquitoes as seen in Fig.(3) (b), (c) and (d) respectively.

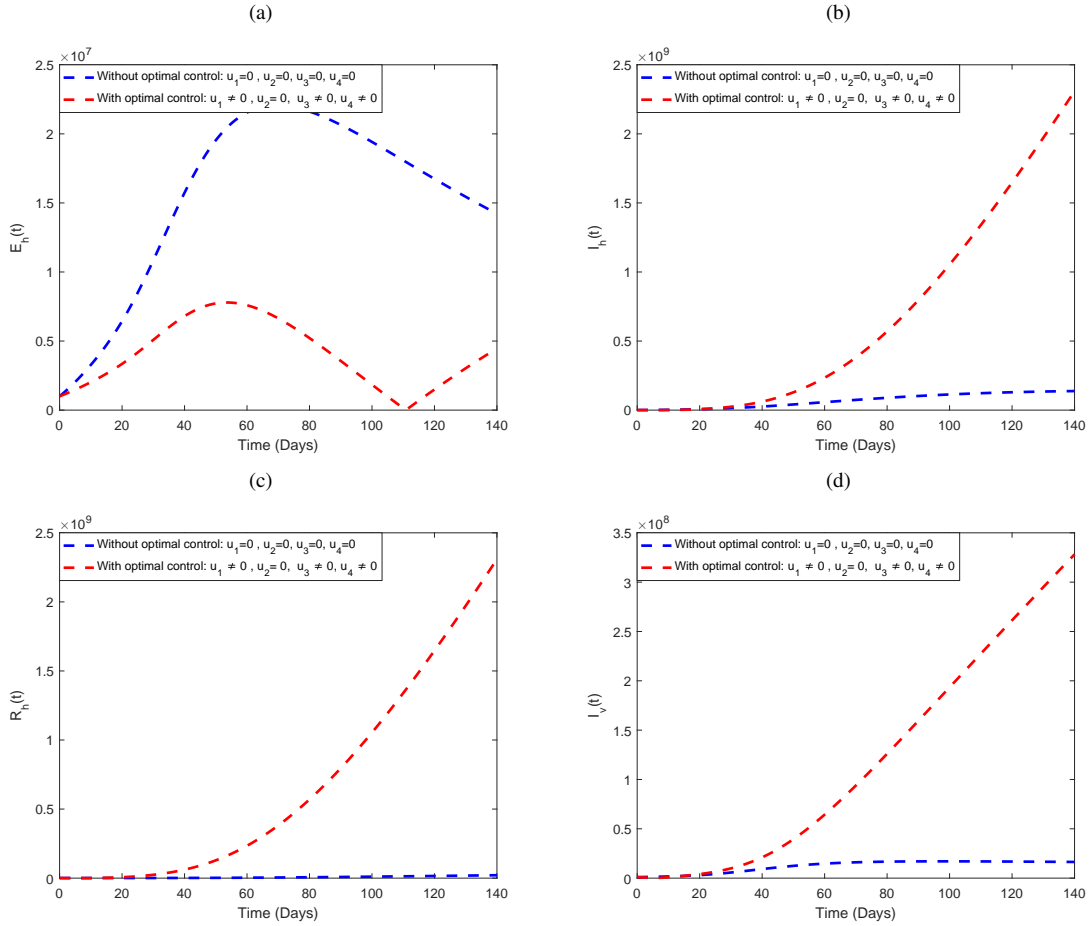


Fig. 3. (a), (b), (c), and (d) represent the behaviors of exposed, infected and recovered humans and infected mosquitoes respectively. Dashed blue line represents system without control ($u_1(t) = 0, u_2(t) = 0, u_3(t) = 0, u_4(t) = 0$) and Dashed red line shows the system with control ($u_1(t) \neq 0, u_2(t) = 0, u_3(t) \neq 0, u_4(t) \neq 0$)

C. Combination of $u_1(t), u_2(t), u_4(t)$ together when $u_3(t) = 0$.

In Fig.(4) (a), (b) the controls $u_1(t), u_2(t), u_4(t)$ are used together while $u_3(t) = 0$. Clearly, there is a significant effect between the states with control and those without control. The number of exposed humans, $E_h(t)$, decreased very fast after day 50 of the implementation process up to day 110, then it started to increase, as in Fig.(4) (a). Similarly, the number of infected humans, $I_h(t)$, begins to decrease after day 50 see Fig.(4) (b). In addition to that, Fig.(4) (c) and (d) indicate that the recovered humans and the number of infected mosquitoes increased respectively.

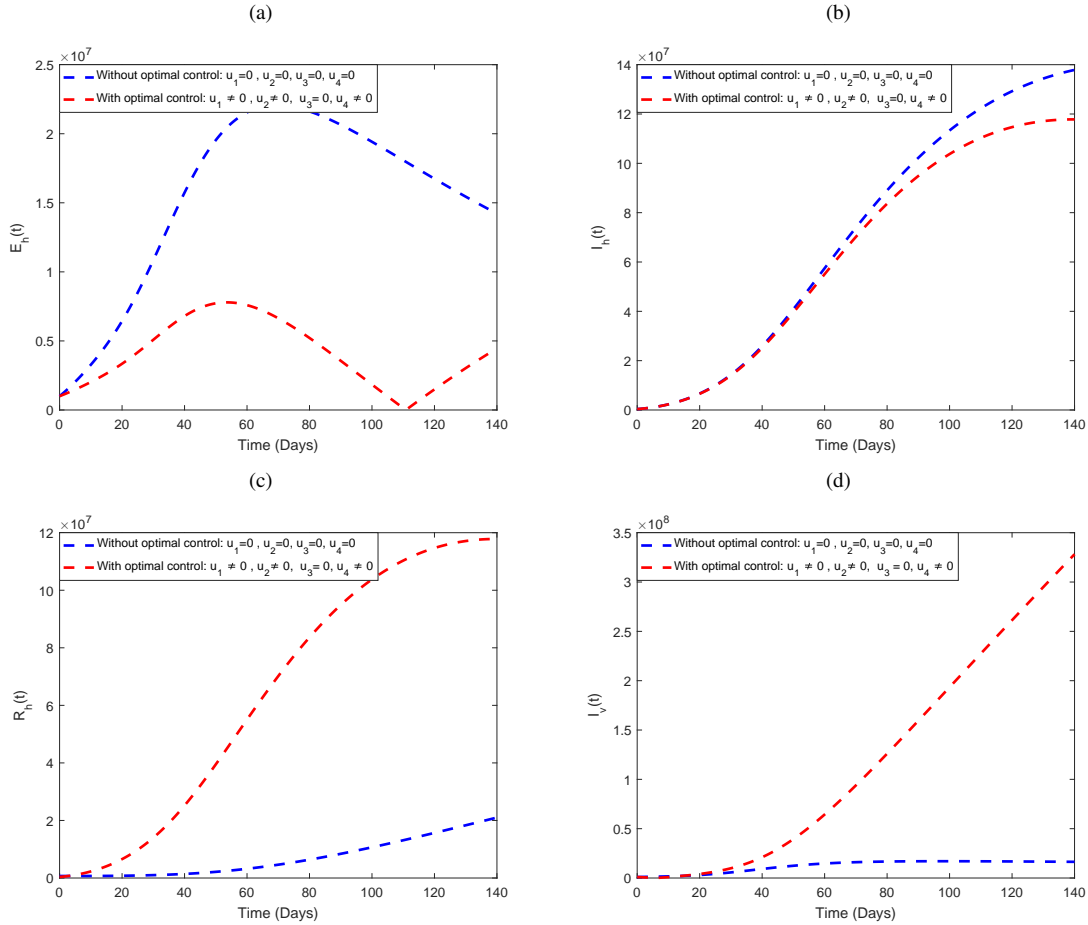


Fig. 4. (a), (b), (c), and (d) represent the behaviors of exposed, infected and recovered humans and infected mosquitoes respectively. Dashed blue line represents system without control ($u_1(t) = 0, u_2(t) = 0, u_3(t) = 0, u_4(t) = 0$) and Dashed red line shows the system with control ($u_1(t) \neq 0, u_2(t) \neq 0, u_3(t) = 0, u_4(t) \neq 0$.)

D. Combination of $u_1(t), u_2(t), u_3(t)$ together when $u_4(t) = 0$

This strategy combines the controls $u_1(t), u_2(t), u_3(t)$ and setting $u_4(t) = 0$. From the below graphs, Fig.(5) (a) indicates that the strategy is effective in reducing the number of exposed humans until after day 110, then starts to increase. From Fig.(5) (b), the number of infected humans has increased. Additionally, Fig.(5) (c) shows that this strategy shows increasing the number of recovered humans quickly recovered. And Fig.(5) (d), shows there is no effect of this strategy on the number of infected mosquitoes.

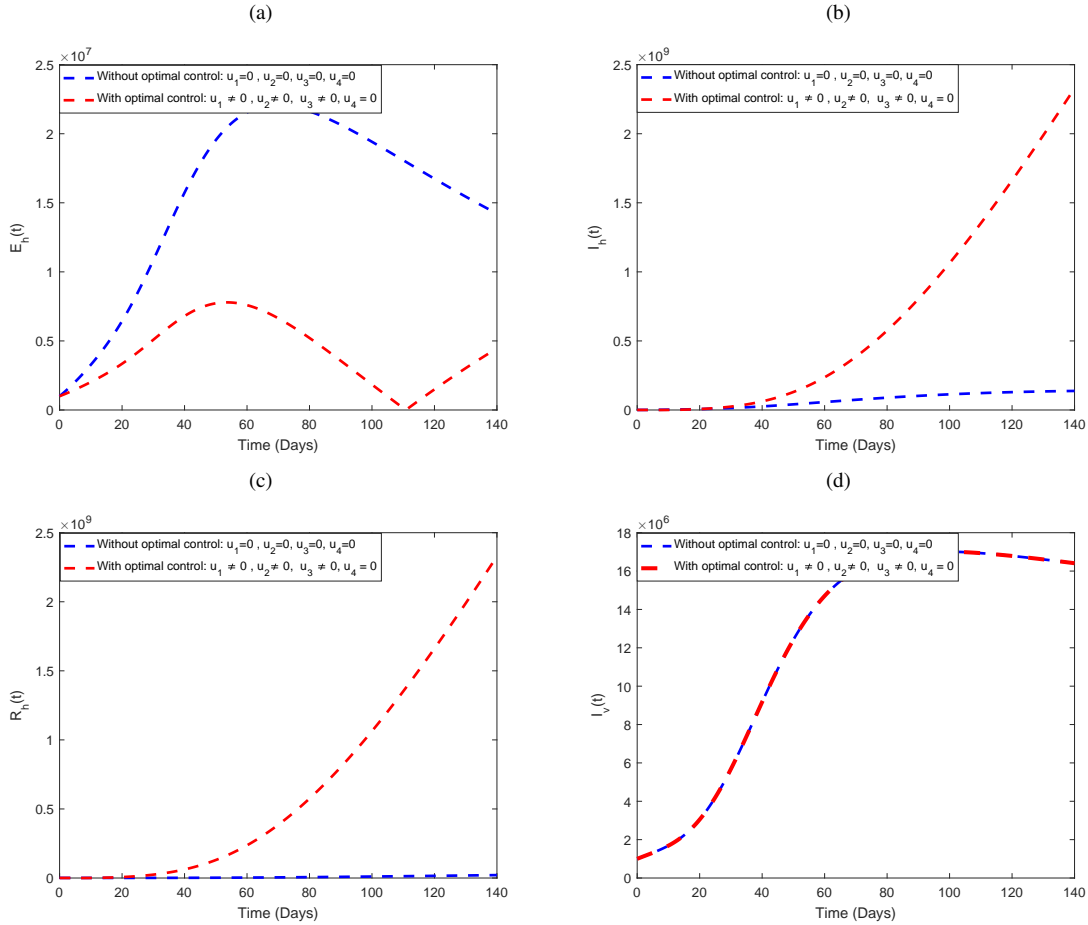


Fig. 5. (a), (b), (c), and (d) represent the behaviors of exposed, infected and recovered humans and infected mosquitoes respectively. Dashed blue line represents system without control ($u_1(t) = 0, u_2(t) = 0, u_3(t) = 0, u_4(t) = 0$) and Dashed red line shows the system with control ($u_1(t) \neq 0, u_2(t) \neq 0, u_3(t) \neq 0, u_4(t) = 0$.)

E. Combination of $u_1(t), u_2(t)$ together when $u_3(t) = 0, u_4(t) = 0$.

This strategy combines the controls $u_1(t), u_2(t)$, and setting $u_3(t) = 0, u_4(t) = 0$. From the below graphs, Fig.(6) (a) indicates that the strategy is effective in reducing the number of exposed humans until after day 110, then starts to increase. From Fig.(6) (b), the number of infected humans has decreased after day 50. Additionally, Fig.(6) (c) shows that this strategy shows increasing the number of recovered humans quickly recovered. And Fig.(6) (d), shows there is no effect of this strategy on the number of infected mosquitoes.

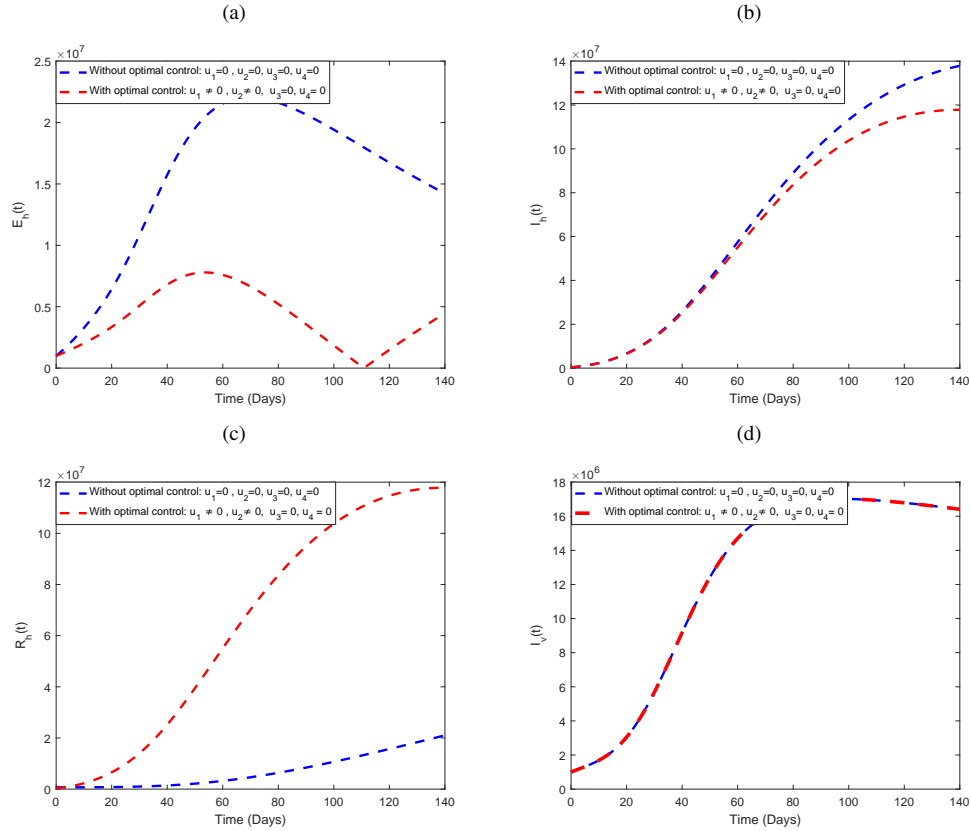


Fig. 6. (a), (b), (c), and (d) represent the behaviors of exposed, infected and recovered humans and infected mosquitoes respectively. Dashed blue line represents system without control ($u_1(t) = 0, u_2(t) = 0, u_3(t) = 0, u_4(t) = 0$) and Dashed red line shows the system with control ($u_1(t) \neq 0, u_2(t) \neq 0, u_3(t) = 0, u_4(t) = 0$.)

F. Combination of $u_1(t), u_3(t)$ together when $u_2(t) = 0, u_4(t) = 0$.

This strategy combines the controls $u_1(t), u_3(t)$ and setting $u_2(t), u_4(t) = 0$. From the graph below, Fig.(7) (a) indicates that the strategy is effective in reducing the number of exposed humans until after day 110, then starts to increase. From Fig.(7) (b) the number of infected humans is increased. Moreover, Fig.(7) (c) shows that this strategy shows increasing the number of recovered humans. And Fig.(7) (d), shows there is no effect of this strategy on the number of infected mosquitoes.

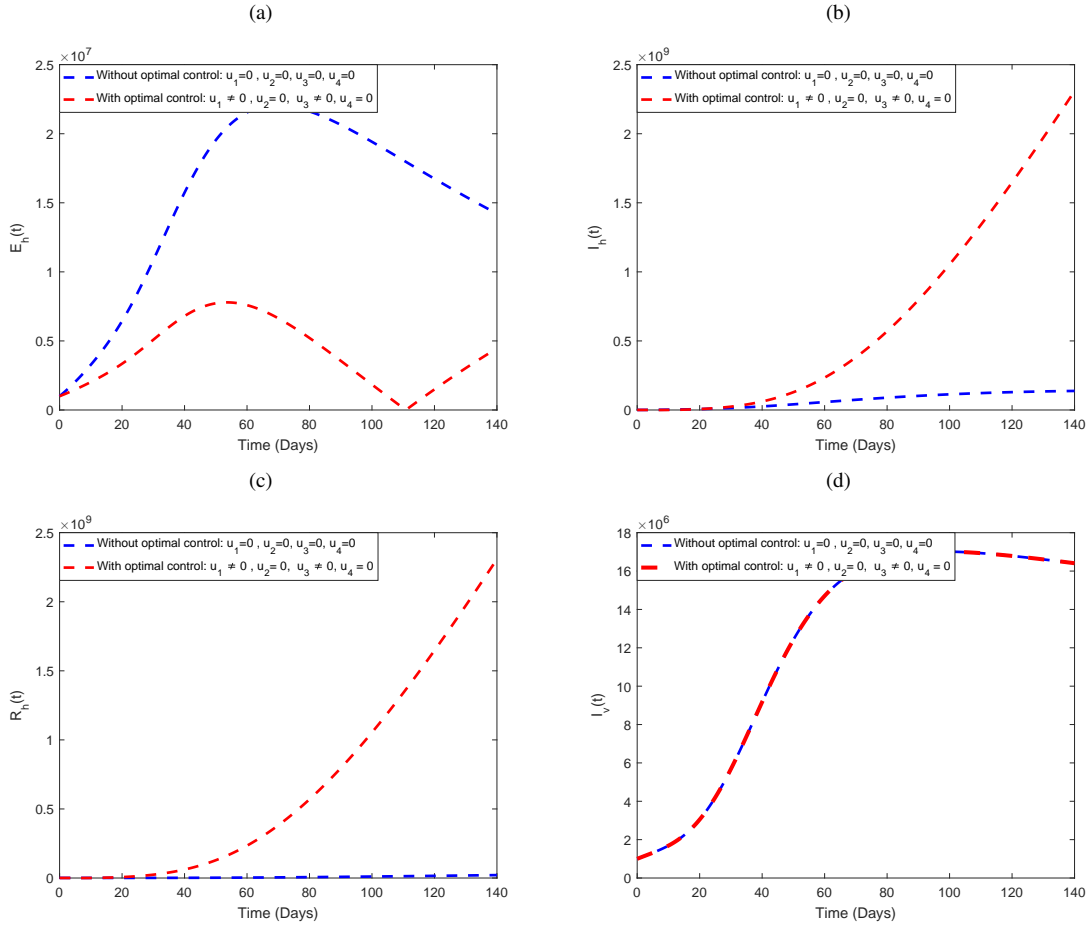


Fig. 7. (a), (b), (c), and (d) represent the behaviors of exposed, infected and recovered humans and infected mosquitoes respectively. Dashed blue line represents system without control ($u_1(t) = 0, u_2(t) = 0, u_3(t) = 0, u_4(t) = 0$) and Dashed red line shows the system with control ($u_1(t) \neq 0, u_2(t) = 0, u_3(t) \neq 0, u_4(t) = 0$.)

G. Combination of $u_1(t), u_4(t)$ together when $u_2(t) = 0, u_3(t) = 0$.

With this strategy, we combined the use of $u_1(t), u_4(t)$ and set $u_2(t) = 0, u_3(t) = 0$. From the graph in Fig.(8)(a), this strategy decreases the number of exposed humans until after day 110, and the number with control begins to increase again. From Fig.(8) (b), this strategy has no effect on the number of infected humans. On the other hand, this strategy increases the number of recovered as in Fig.(8)(c). Also, Fig.(8)(d), shows that the number of infected mosquitoes is increasing. This means that this strategy is not good for controlling malaria.

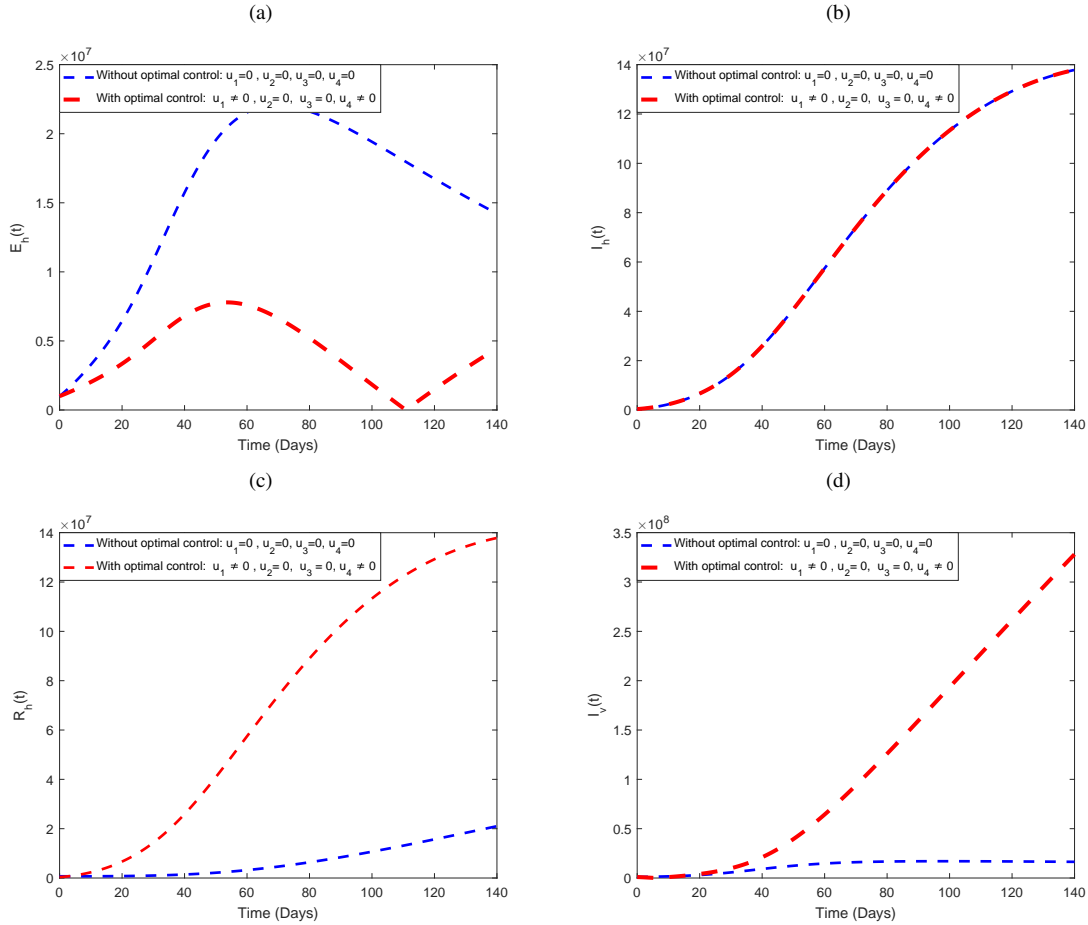


Fig. 8. (a), (b), (c), and (d) represent the behaviors of exposed, infected and recovered humans and infected mosquitoes respectively. Dashed blue line represents system without control ($u_1(t) = 0, u_2(t) = 0, u_3(t) = 0, u_4(t) = 0$) and Dashed red line shows the system with control ($u_1(t) \neq 0, u_2(t) = 0, u_3(t) = 0, u_4(t) \neq 0$.)

H. Combination of $u_3(t), u_4(t)$ together when $u_1(t) = 0, u_2(t) = 0$.

In this strategy, we combined the use of $u_3(t), u_4(t)$ and set $u_1(t) = 0, u_2(t) = 0$. This control strategy shows no difference between the number of exposed humans with control and without control this can be seen in Fig.(9)(a). However, from Fig.(9)(b), (c) and (d), this strategy significantly increases the number of infected humans, the number of recovered humans and also increases the number of infected mosquitoes, respectively, until the end of the simulation period.

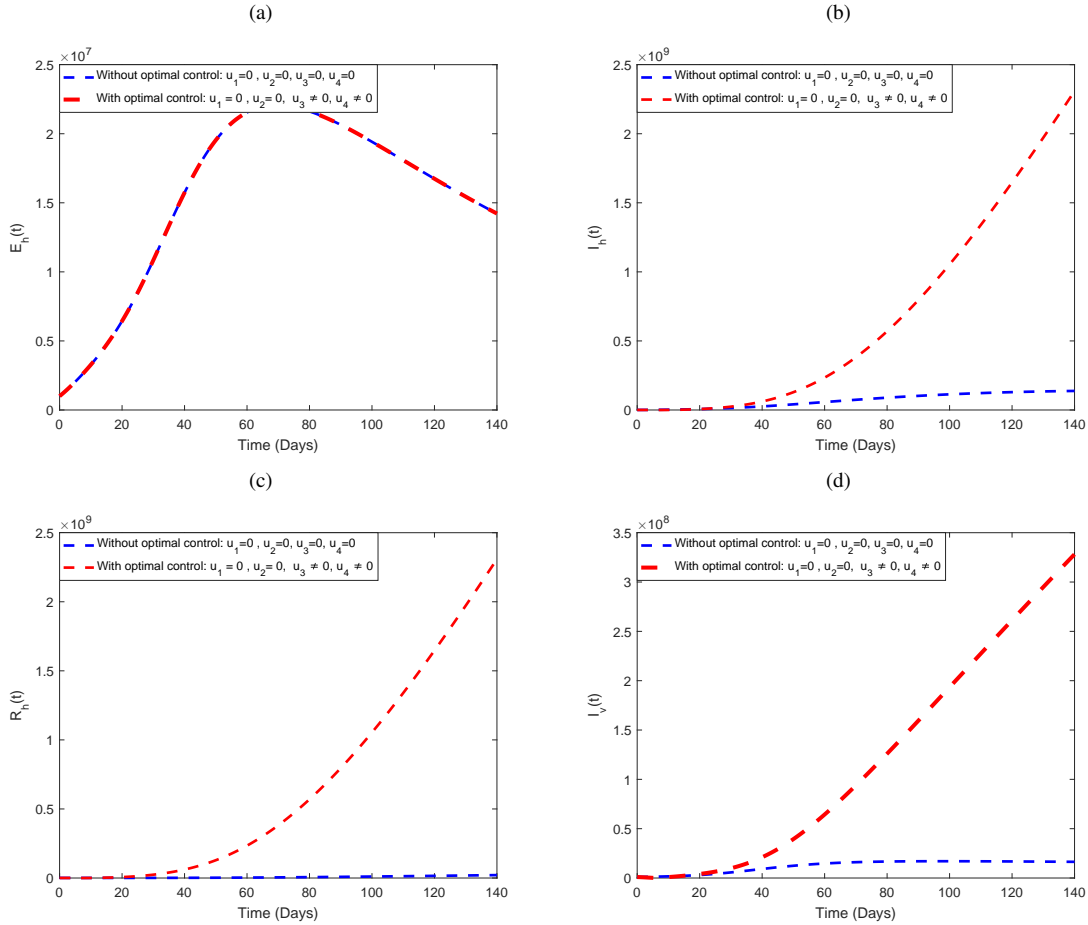


Fig. 9. (a), (b), (c), and (d) represent the behaviors of exposed, infected and recovered humans and infected mosquitoes respectively. Dashed blue line represents system without control ($u_1(t) = 0, u_2(t) = 0, u_3(t) = 0, u_4(t) = 0$) and Dashed red line shows the system with control ($u_1(t) = 0, u_2(t) = 0, u_3(t) \neq 0, u_4(t) \neq 0$.)

I. Combination of $u_2(t), u_3(t)$ together when $u_1(t) = 0, u_4(t) = 0$.

We combined in this strategy the use of $u_2(t), u_3(t)$ and set $u_1(t) = 0, u_4(t) = 0$. This strategy shows no difference between the number of exposed humans with control and without control and the number of infected mosquitoes as in Fig.(10) (a) and (d). Besides, Fig.(10) (b) and (c), show increases in the number of infected humans and the number of recovered humans respectively, until the end of the simulation period.

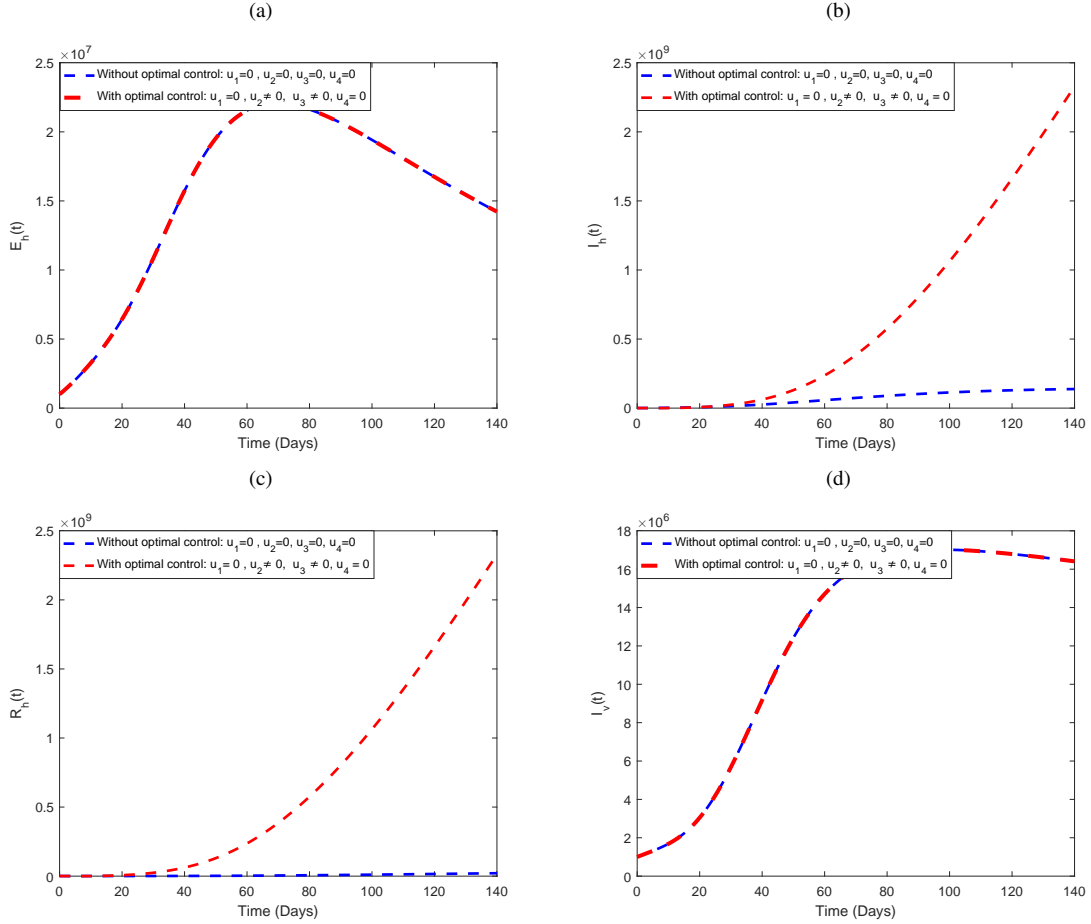


Fig. 10. (a), (b), (c), and (d) represent the behaviors of exposed, infected and recovered humans and infected mosquitoes respectively. Dashed blue line represents system without control ($u_1(t) = 0, u_2(t) = 0, u_3(t) = 0, u_4(t) = 0$) and Dashed red line shows the system with control ($u_1(t) = 0, u_2(t) \neq 0, u_3(t) \neq 0, u_4(t) = 0$.)

J. Combination of $u_2(t), u_4(t)$ together when $u_1(t) = 0, u_3(t) = 0$.

In this strategy, we combined $u_2(t), u_4(t)$ and set $u_1(t), u_3(t)$. From Fig.(11) (a) it can be seen that this strategy does not affect the number of exposed humans. However, from Fig.(11)(b), (c) and (d), this strategy significantly increases the number of infected humans, the number of recovered humans and also increases the number of infected mosquitoes, respectively, until the end of the simulation period, as in Fig.(10)(b), (c) and (d) respectively.

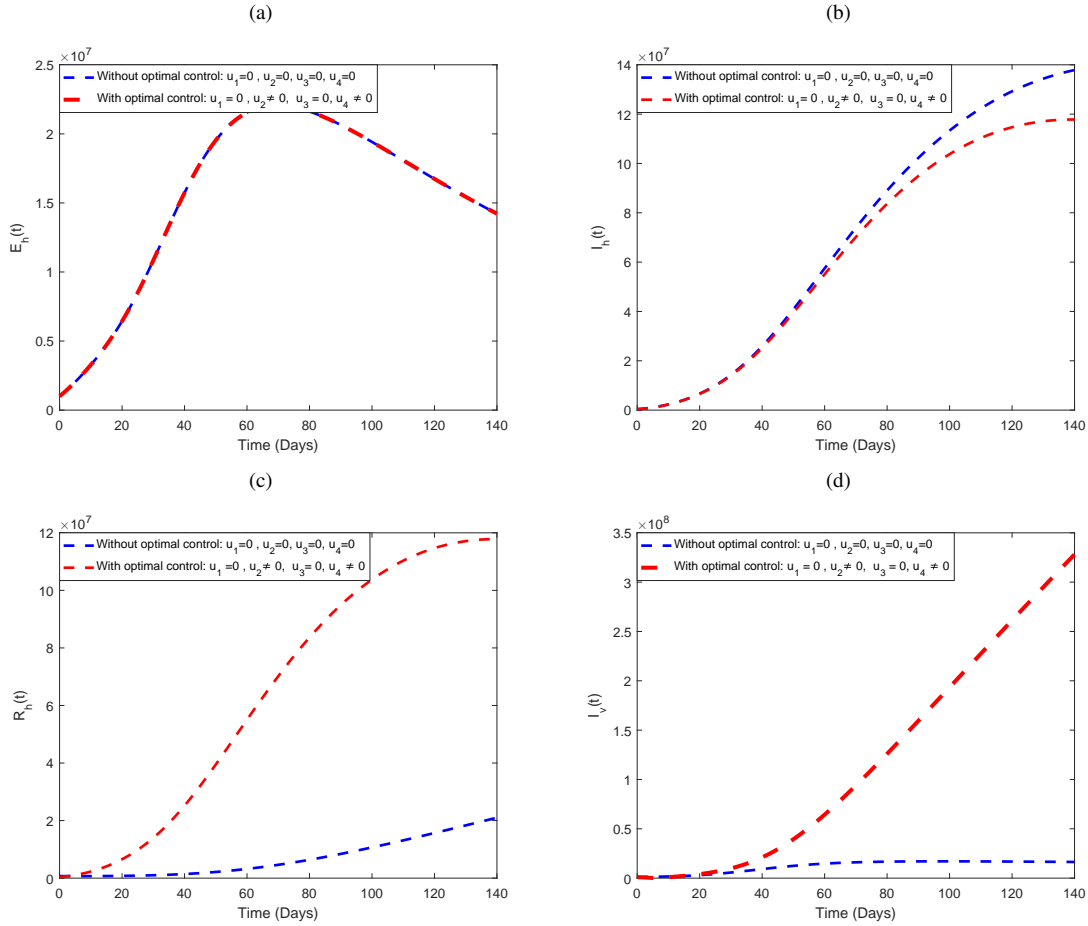


Fig. 11. (a), (b), (c), and (d) represent the behaviors of exposed, infected and recovered humans and infected mosquitoes respectively. Dashed blue line represents system without control ($u_1(t) = 0, u_2(t) = 0, u_3(t) = 0, u_4(t)$) and Dashed red line shows the system with control ($u_1(t) = 0, u_2(t) \neq 0, u_3(t) = 0, u_4(t) \neq 0$.)

K. Combination of $u_1(t), u_2(t), u_3(t)$ and, $u_4(t)$ together:

This is the strategy of using all controls together. The graphs for this strategy are shown in Fig.(12)(a), (b), (c) and (d). Clearly, there is a significant effect between the states with and without control. The number of exposed humans, $E_h(t)$, starts to decrease very fast after day 75, indicating that the control measures are effective in reducing exposure. See Fig.(12)(a). In Fig.(12)(b), the number of infected humans, $I_h(t)$ the growth of infections is significantly reduced, peaking earlier and at a much lower level, then starting to decline, showing the impact of control interventions on curbing malaria spread. Also, from Fig.(12) (c), this suggests that with all optimal control strategies, people recover faster, but since fewer people get infected overall, the total number of recoveries can decrease after peaking. Furthermore, Fig.(12) (d) shows that control measures significantly reduce the spread among vectors, which is crucial for malaria control. The simulation results clearly demonstrate that applying optimal control measures significantly reduces the impact of the disease on both human and vector populations and increases the number of recovered humans.

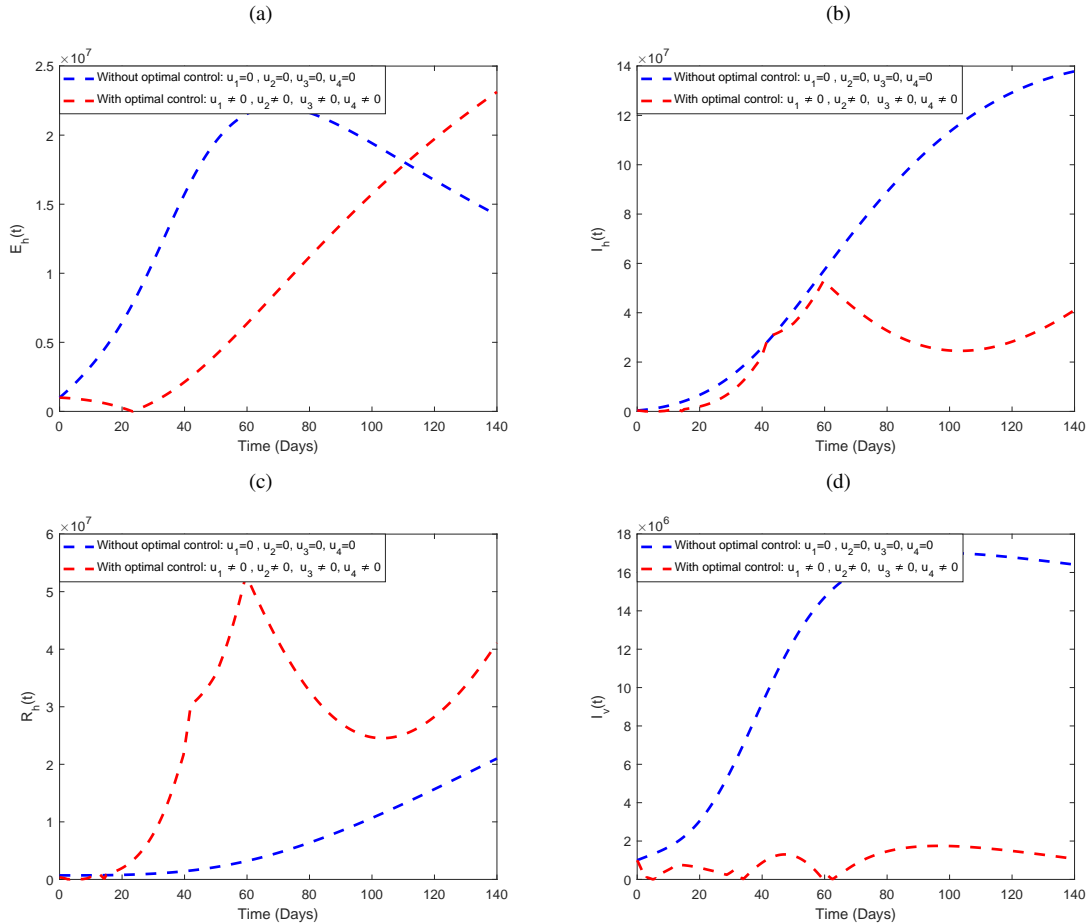


Fig. 12. (a), (b), (c), and (d) represent the behaviors of exposed, infected and recovered humans and infected mosquitoes respectively. Dashed blue line represents system without control ($u_1(t) = 0, u_2(t) = 0, u_3(t) = 0, u_4(t) = 0$) and Dashed red line shows the system with control ($u_1(t) \neq 0, u_2(t) \neq 0, u_3(t) \neq 0, u_4(t) \neq 0$.)

7. Conclusion

In this paper, we studied the standard SEIR-SEI ordinary differential equation mathematical model for malaria transmission. The fundamental properties of the model were investigated, \mathcal{R}_0 is also obtained. Thus, when $\mathcal{R}_0 > 1$, the disease persists in the area and when $\mathcal{R}_0 < 1$ the disease will die out. Furthermore, four control strategies; $u_1(t), u_2(t), u_3(t)$ and $u_4(t)$ were included in the model to reduce and control the disease in the human population. According to our optimal control numerical simulation results, the best strategy for reducing and controlling the number of exposed, infected humans and infected mosquitoes as well as increasing the number of recovered humans is the use of all the four control strategies together, which is highly beneficial in flattening the epidemic curves, shortening the duration of the outbreak, and lessening the burden on the healthcare system. These findings underscore the importance of timely and well-designed public health interventions in disease outbreak scenarios.

ACKNOWLEDGEMENTS

Appendix

These graphs shows the implementation schedule of malaria four optimal control strategies based on our optimal control analysis, related to Fig.(2) to Fig.(12) in Section 6 respectively.

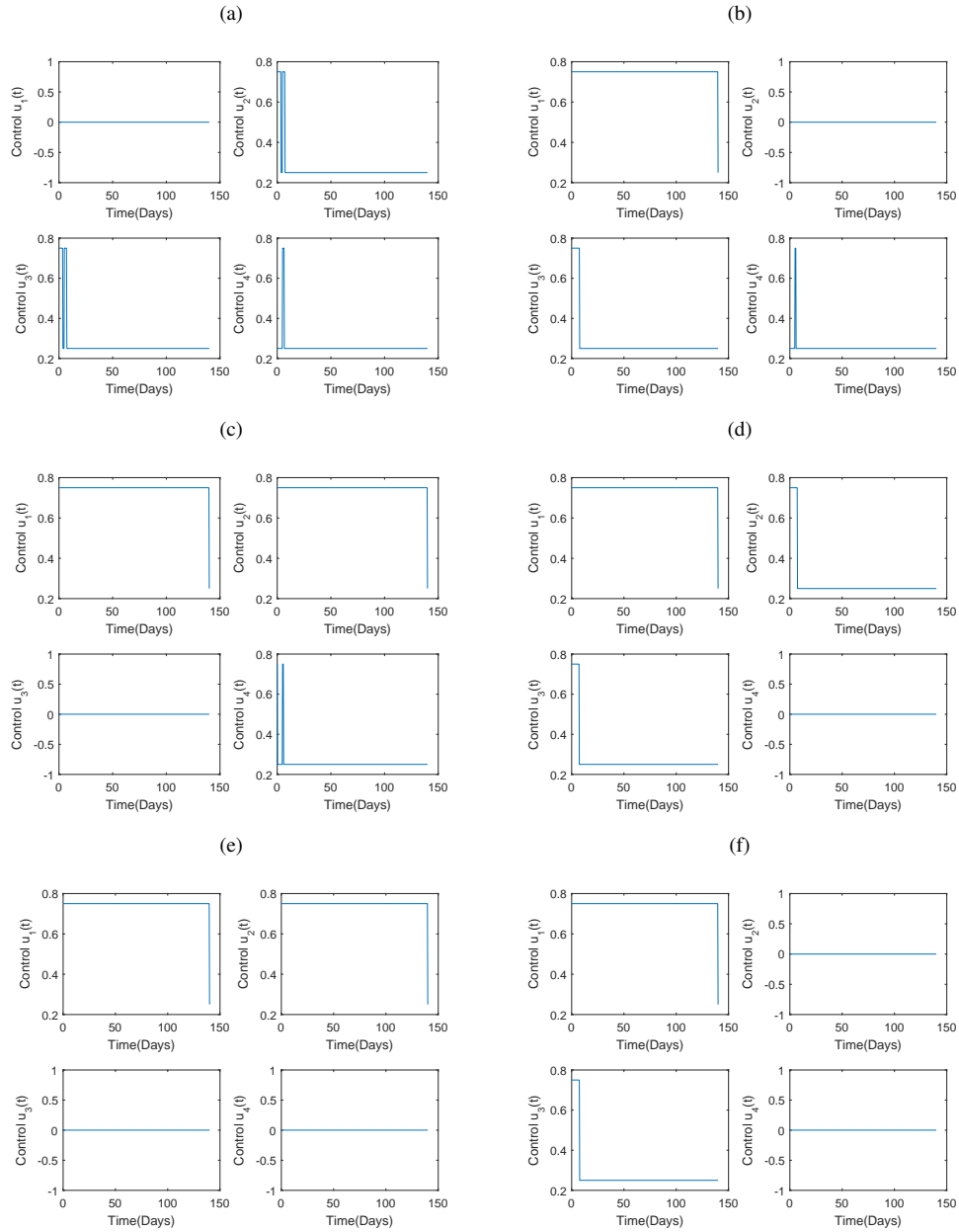


Fig. 13. Graphs shows the Implementation Schedule of Malaria four optimal control Strategies.

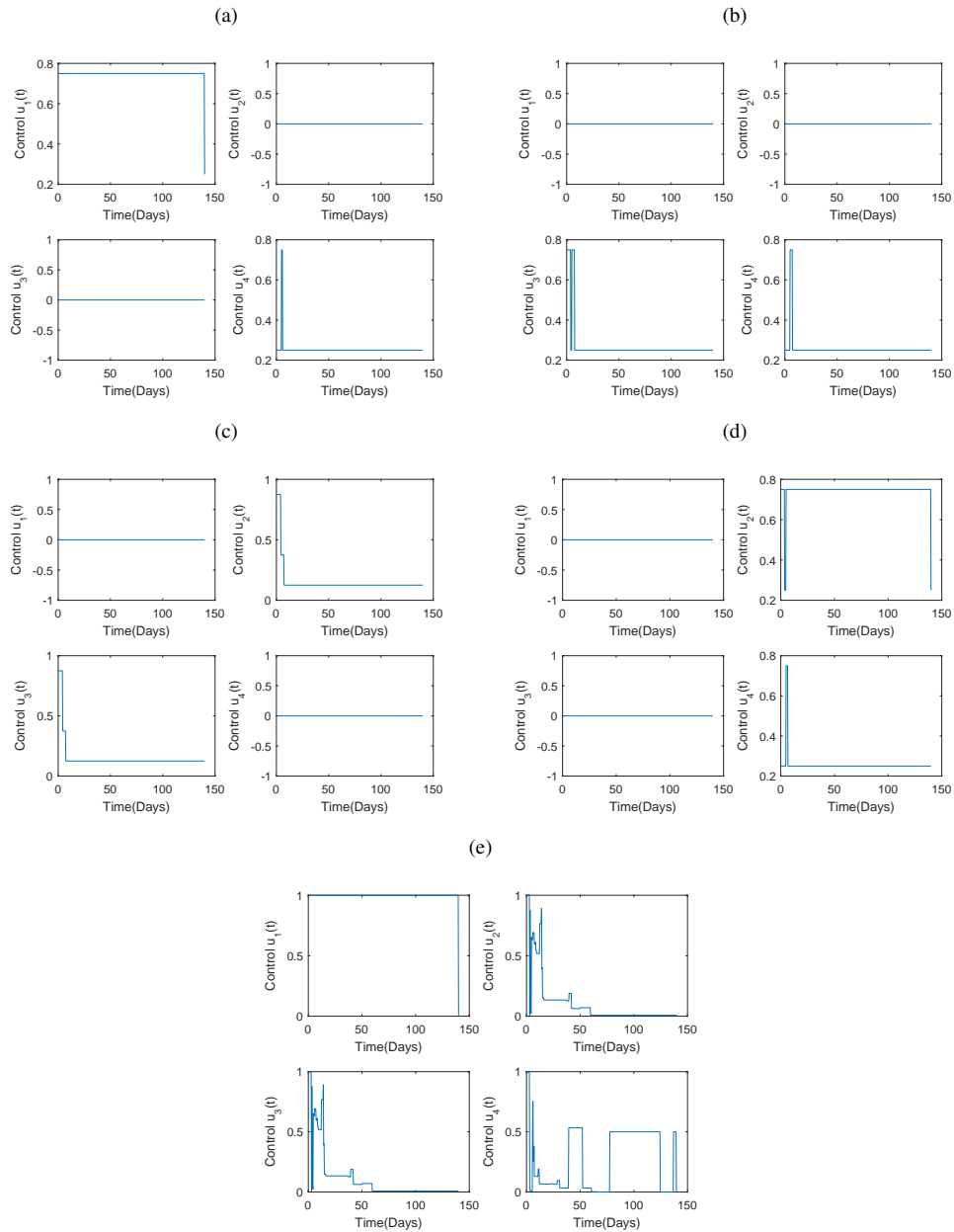


Fig. 14. Graphs shows the Implementation Schedule of Malaria four optimal control Strategies.

REFERENCES

- [1] WHO. Malaria report available at: <https://www.who.int/teams/global-malaria-programme/reports/world-malaria-report-2024>
- [2] WHO. Malaria report available at: <https://www.who.int/news-room/fact-sheets/detail/malaria> -11 Dec 2024
- [3] Marsh K, Forster D, Waruiru C, Mwangi I, Winstanley M, Marsh V, Newton C, Winstanley P, Warn P, Peshu N, et al. Indicators of life-threatening malaria in African children. *New England journal of medicine*,(1995) 332(21):1399-1404.
- [4] Babiker, Hamza A., Amal A.H Gadalla, and Lisa C. Ranford-Cartwright. The role of asymptomatic P. The role of asymptomatic *P.falciparum* parasitaemia in the evolution of antimalarial drug resistance in areas of seasonal transmission. *Drug Resist Updates*. (2013),16(2):1-9.
- [5] World malaria report 2021 available at: <https://www.who.int/publications/i/item/9789240040496>
- [6] Malaria world report 2018, available at:<https://apps.who.int/iris/bitstream/handle/10665/275867/9789241565653-eng.pdf?ua=1>
- [7] Okosun, K.O., Rachid, O. and Marcus, N. Optimal control strategies and cost-effectiveness analysis of a malaria model,*BioSystems* .(2013),111(2):83-101.
- [8] Mwangi, G. G., Haario, H., and Capasso, V. Optimal control problems of epidemic systems with parameter uncertainties: application to a malaria two-age-classes transmission model with asymptomatic carriers,*Mathematical Biosciences*.(2015), 261:1-12.
- [9] Romero-Leiton, J. P., Montoya-Aguilar, J. M., and Ibargüen-Mondragón, E. An optimal control problem applied to malaria disease in Colombia,*Applied Mathematical Sciences*,(2018),12(6):279-292.
- [10] Mojeeb, A. L., Yang, C., and Adu, I. K. Mathematical Model of Malaria Transmission with Optimal Control in Democratic Republic of the Congo. *Global Journal of Science Frontier Research*, (2019), 19(1):2249-4626.
- [11] Garira, W., and Mathebula, D. A coupled multiscale model to guide malaria control and elimination,*Journal of Theoretical Biology* ,(2019),475: 34-59.
- [12] Lee, T. E., and Penny, M. A. Identifying key factors of the transmission dynamics of drug-resistant malaria. *Journal of Theoretical Biology*, (2019),462: 210-220.
- [13] Okosun, K. O. Optimal Control Analysis Of Malaria-Schistosomiasis Co-Infection Dynamics. *Mathematical Biosciences And Engineering* (2017),14(2): 377-405.
- [14] Dembele, B., and Yakubu, A. A. Controlling Imported Malaria Cases In The United States Of America. *Mathematical Biosciences And Engineering*,(2017),14(1):95-109.
- [15] Mwamtobe, P. M., Simelane, S. M., Abelman, S., and Tchuenche, J. M. Optimal control of intervention strategies in malaria-tuberculosis co-infection with relapse, *International Journal of Biomathematics*,(2018),11(02): 1850017.
- [16] Cai, L., Li, X., Tuncer, N., Martcheva, M., and Lashari, A. A. Optimal control of a malaria model with asymptomatic class and superinfection. *Mathematical Biosciences*, (2017),288: 94-108.
- [17] Blayneh, K., Cao, Y., and Kwon, H. D. Optimal control of vector-borne diseases: Treatment and prevention. *Discrete and Continuous Dynamical Systems-B*,(2009),11(3):587-611.
- [18] Rafikov, M., Bevilacqua, L., and Wyse, A. P. P. Optimal control strategy of malaria vector using genetically modified mosquitoes. *Journal of Theoretical Biology*, (2009).258(3):418-425.
- [19] Keno, Temesgen Duressa, Lemesa Bedjisa Dano, and Gamachu Adugna Ganati. Optimal Control and Cost-Effectiveness Strategies of Malaria Transmission with Impact of Climate Variability. *Journal of Mathematics* (2022), no. 1: 5924549.
- [20] Jaleta, Sisay Fikadu, Gemechis File Duressa, and Chernet Tuge Deressa. "A mathematical modeling and optimal control analysis of the effect of treatment-seeking behaviors on the spread of malaria." *Frontiers in Applied Mathematics and Statistics*. 11 (2025): 1552384.
- [21] Mojeeb, A. L., and Jinhui Li. "Analysis of a vector-bias malaria transmission model with application to Mexico, Sudan and Democratic Republic of the Congo." *Journal of Theoretical Biology* 464 (2019): 72-84.
- [22] Li, Jinhui, A. L. Mojeeb, and Zhidong Teng. "Optimal control analysis of a malaria transmission model with applications to Democratic Republic of Congo." *Nonlinear Analysis: Modelling and Control* 28, no. 5 (2023): 883-905.
- [23] Adu, Isaac Kwasi, Fredrick Asenso Wireko, Sacrifice Nana-Kyere, Ebenezer Appiagyei, Mojeeb AL-Rahman EL-Nor Osman, and Joshua Kiddy K. Asamoah. "Modelling the dynamics of Ebola disease transmission with optimal control analysis." *Modeling Earth Systems and Environment* 10, no. 4 (2024): 4731-4757.

- [24] Aguilar, J. M., Romero-Leiton, J. P., de Urcuqui, Y. T. S. M., and Ibargüen-Mondragón, E.E. Qualitative analysis of a mathematical model applied to malaria disease transmission in Tumaco (Colombia). *Applied Mathematical Sciences*,(2018),12(5):205-217.
- [25] Mojeeb, A., Adu, I. K., and Yang, C. A Simple SEIR Mathematical Model of Malaria Transmission. *Asian Research Journal of Mathematics*,(2017),1-22.
- [26] Chitnis, N. R. Using Mathematical Models in Controlling the Spread of Malaria, University of Arizona,(2005).
- [27] Li J, Mojeeb AL, Teng Z. Optimal control analysis of a malaria transmission model with applications to Democratic Republic of Congo. *Nonlinear Analysis: Modelling and Control*. 2023 Jun 30;28(5):883-905.
- [28] Hirsch, W. M., Hanisch, H., and Gabriel, J. P. Differential equation models of some parasitic infections: methods for the study of asymptotic behavior. *Communications on Pure and Applied Mathematics*,(1985), 38(6):733-753.
- [29] Van den Driessche, P., and Watmough, J. Reproduction numbers and sub-threshold endemic equilibria for compartmental models of disease transmission. *Mathematical Biosciences*,(2002),180(1-2):29-48.
- [30] Pontryagin L.S.,Boltyanskii V.G.,Gamkrelide R.V., and Mishchenko E.F. The mathematical theory of optimal processes. Wiley, New York (1962).